







Cite this: *Sens. Diagn.*, 2022, **1**, 1198

# Metal organic framework encapsulated tamavidin-Gluc reporter: application in COVID-19 spike antigen bioluminescent immunoassay†

Sherwin Reyes, <sup>ab</sup> Emily Rizzo,<sup>a</sup> Albert Ting,<sup>a</sup> Emre Dikici, <sup>ab</sup>  
 Sylvia Daunert <sup>abc</sup> and Sapna K. Deo <sup>\*ab</sup>

Enzyme linked immunosorbent assay (ELISA) is one of the most utilized serological methods to diagnose and identify etiologic agents of many infectious diseases and other physiologically important analytes. ELISA can be used either alone or adjunct to other diagnostic methods such as molecular arrays, and other serological techniques. Most ELISA assays utilize reagents that are proteinaceous in nature, which are not very stable and require cold-chain transport systems. Development of a desirable immunoassay requires stability of reagents used and its ability to be stored at room temperature without sacrificing the activity of the reagents or the protein of interest. Metal organic frameworks (MOFs) are a rapidly emerging and evolving class of porous polymeric materials used in a variety of biosensor applications. In this study, we introduce the use of MOFs to stabilize a universal reporter fusion protein, specifically, avidin-like protein (Tam-avidin2) and the small bioluminescent protein *Gaussia luciferase* (Gluc) forming the fusion reporter, tamavidin2-Gluc (TA2-Gluc). This fusion protein serves as a universal reporter for any assays that utilize biotin-avidin binding strategy. Using SARS-CoV2 S1 spike antigen as the model target antigen, we demonstrated that encapsulation of TA2-Gluc fusion protein using a nano-porous material, zeolitic imidazolate framework-8 (ZIF-8), allows us to store and preserve this reporter protein at room temperature for over 6 months and use it as a reporter for an ELISA assay. Our optimized assay was validated demonstrating a 0.26  $\mu\text{g mL}^{-1}$  limit of detection, high reproducibility of assay over days, detection of spiked non-virulent SARS-COV2 pseudovirus in real sample matrix, and detection in real COVID-19 infected individuals. This result can lead to the utilization of our TA2-Gluc fusion protein reporter with other assays and potentially in diagnostic technologies in a point-of-care setting.

Received 15th August 2022,  
 Accepted 29th August 2022

DOI: 10.1039/d2sd00145d

[rsc.li/sensors](https://rsc.li/sensors)

## 1. Introduction

Quantitative, accurate, specific, sensitive, rapid, and field deployable immunoassays are currently in-demand due to increasing cases of new and re-emerging infectious diseases. A variety of approaches including agglutination testing,<sup>1</sup> immunofluorescent assay (IFA),<sup>2,3</sup> radioimmunoassay (RIA),<sup>4</sup> enzyme-linked immunosorbent assays (ELISA), and other immunoassay platforms have come a long way for the rapid detection of antigens or antibodies corresponding to such infectious agents.<sup>5</sup> Amongst these methods, ELISA has been

the go-to method in a clinical setting due to its simple procedure, specificity, short turn-around time (TAT), and high sensitivity.<sup>4,6</sup> A typical ELISA utilizes an enzyme linked antigen or antibody conjugates. The formation of product of the enzymatic reaction provides for the generation of the signal that can be correlated with the target analyte/pathogen in a sample.<sup>6</sup> Although RIA is one of the most sensitive immunoassay methods, owing to the use of radioactive labels, its application in diagnostic testing is now diminished. New ELISA and immunoassays using labels such as bioluminescent proteins termed bioluminescent immunoassay (BIA) and chemiluminescent substrates have achieved sensitivity comparable to RIA.<sup>4,7,8</sup> Specifically, horseradish peroxidase label combined with chemiluminescent substrates and bioluminescent proteins such as *Gaussia luciferase* (Gluc), *Renilla luciferase* (Rluc), and *aequorin* have become popular labels for the design of new immunoassays. The use of bioluminescent proteins, which are small and can be expressed in bacteria, provides an additional advantage to create genetic fusions, allowing for

<sup>a</sup> Department of Biochemistry and Molecular Biology, University of Miami – Miller School of Medicine, Miami, FL 33136, USA. E-mail: [SDeo@med.miami.edu](mailto:SDeo@med.miami.edu)

<sup>b</sup> The Dr. John T. McDonald Foundation Bionanotechnology Institute of University of Miami, Miami, FL 33136, USA

<sup>c</sup> Clinical and Translational Science Institute of University of Miami, FL 33136, USA

† Electronic supplementary information (ESI) available. See DOI: <https://doi.org/10.1039/d2sd00145d>



better reproducibility of reagents and conjugate preparation. Our laboratory recently reported the construction and bacterial expression of a fusion protein composed of the biotin-binding protein tamavidin 2 (TA2) and bright luminescent reporter Gluc to generate the fusion protein TA2-Gluc.<sup>9</sup> TA2 protein provides for binding to biotin and Gluc provides for signal generation with high signal/noise ratio upon binding of TA2 to biotin. We hypothesize that this fusion protein can serve as a universal reporter protein since it can be employed as a reporter in many assay types, including immunoassays, where avidin-biotin type binding is commonly utilized in an assay design. We have demonstrated that this fusion protein can be prepared in large quantities using bacterial expression and purification system and yields high bioluminescent signal.<sup>9</sup> We also showed its utility as a reporter in DNA hybridization assays previously.<sup>9</sup> Now we show that this reporter protein could be easily employed as a label in immunoassays for the development of highly sensitive, accurate, and rapid immunoassays for targets of interest such as pathogens. An additional characteristic that is desired in any immunoassay development is the stability of the reagents used and the ability to store them at room temperature or higher temperatures, to avoid the use of refrigeration. In that regard, lyophilization based approaches with different cryoprotectants are commonly used to impart stability to proteins for storage at room temperature. However, this method does not always yield desired stability without sacrificing the activity of the reagent/protein of interest. Therefore, additional methods such as encapsulation with polymers<sup>10,11</sup> and metal-organic frameworks<sup>12–14</sup> have been reported. In that regard, in this manuscript we have prepared room temperature stable TA2-Gluc based on encapsulation with metal organic frameworks and showed their application as a label in the design of an immunoassay using COVID-19 spike antigen as the model target analyte. We believe that the creation of a stable, extended shelf-life reporter that is based on universally used avidin-biotin binding and high signal generating bioluminescent protein will find application in a variety of assay designs.

Metal-organic frameworks (MOFs) can be used to preserve and store labile biomolecules such as proteins at room temperature for longer periods.<sup>15–17</sup> MOFs includes different composites of functional materials such as metal nanoparticles, oxides, quantum dots, polyoxometalates polymers, graphene, carbon nanotubes, biomolecules and many preparation methods.<sup>17–32</sup> Amongst MOFs methods, encapsulation pave its way due to its distinct advantage as the MOF pore size is independent of the size of protein and its simplicity. The one step encapsulation method offers the highest level of protection and recyclability, as encapsulated enzymes generally retain better performance during reconstitution because the enzyme is embedded in the MOF particles. There are a multitude of possible combinations for the variety of metal ions, organic linkers, and structural motifs that can provide a great degree of structural diversity, wide range of chemical and physical tunability, low operational cost, good adsorption and desorption

kinetics, ease of handling, and facile functionality.<sup>17,20</sup> Among the many MOF related studies, more than half are related to zeolitic imidazolate framework-8 (ZIF-8) using imidazole as linker.<sup>33</sup> As opposed to infiltration method that uses PVP or alcohol for synthesis, a study conducted by Liang *et al.*,<sup>22</sup> showed that encapsulation using one-pot strategy known as biomimetic mineralization technique can be helpful in maintaining the viability and stability of biomacromolecules under various conditions. In this study, they have encapsulated two different enzymes, urease and horseradish peroxidase, within a ZIF-8 framework and demonstrated that the enzymes were shown to maintain their activity even after being exposed to denaturation conditions. They showed that the ZIF-8 framework was formed simultaneously in water by simply combining the enzymes, 2-methylimidazole (mIM) and zinc acetate. This system is preferable due to its high stability, straight forward production, and excellent performance.<sup>23,34</sup> ZIF-8 is a highly porous type of MOF and an analogue of zeolites and is formed by tetrahedral N atom linkages of metal ions such as Zn<sup>2+</sup> and Co<sup>2+</sup>.<sup>35</sup> Thus, giving rise to a strong bond that provides enormous chemical and thermal stability compared to classic MOFs. Due to its structural flexibility, ZIF-8 possesses good functionality and a wide range of porosities that can be easily manipulated.<sup>32</sup> MOFs ZIF-8, which contains zinc ions, can be used as a protective material for biomolecules to maintain the ability to recognize antibodies or viral proteins on the surface of biosensors stored at ambient and high temperatures.<sup>23,36–38</sup>

In this manuscript, we designed a bioluminescent immunoassay (BIA) using MOFs encapsulated TAM2-Gluc reporter for a model analyte SARS-CoV-2 antigen. Here we describe encapsulation of TA2-Gluc protein with ZIF-8 and demonstrate enhanced room temperature stability of TA2-Gluc for an extended time period. Tamavidin-2 are a group of avidin-like biotin-binding proteins found in the tamogitake mushroom (*Pleurotus comucopiae*), commonly known as “oyster mushroom”. When compared to biotin-binding proteins avidin and streptavidin, TAM2 confers high affinity and is easily produced in soluble form in the bacterial expression system.<sup>39–41</sup> Gluc is a small Renilla-like luciferase (19.9 kDa, emission at 470 nm) derived from copepods (*Gaussia princeps*) that has been cloned since 2002.<sup>42</sup> Gluc, compared to other bioluminescent proteins, gives a high bioluminescent intensity. The encapsulated stable TA2-Gluc protein was employed as a label in the design of a highly sensitive bioluminescent immunoassay for the detection of COVID-19 spike antigen. Coronavirus disease (COVID-19) is an infectious respiratory disease caused by the novel coronavirus strain, SARS-CoV-2, that has spread throughout the world leading to a global pandemic.<sup>43,44</sup> SARS-CoV-2 spreads primarily through droplets discharged from the nose or mouth when an infected person coughs or sneezes and can be detected using immunoassays.<sup>45–47</sup> Therefore, SARS-COV2 antigen serves as a good example of antigen to demonstrate the use of stabilized universal bioluminescent reporter system.



## 2. Experimental section

### 2.1 Materials and methods

**2.1.1 Reagents.** The following reagents were purchased from Southern Biotech (Birmingham, AL): secondary antibody: goat anti-rabbit Ig human ads-BIOT (Cat. No. 4010-08). Primary Antibody: SARS-CoV-2 Spike S1 antibody [HL6] Rb mAb (Cat. No. GTX635654), capture/coating antibody: recombinant SARS-CoV-2 S1 (COVID-19) spike antibody (1A9) (Cat. No. GTX632604) were purchased from GeneTex (Irvine, CA). COVID-19 spike antigen: recombinant SARS-CoV-2 S1 subunit (Cat. No. 230-01101) was purchased from RayBiotech (Peachtree Corners, GA). Coelenterazine (Cat. No. CZ2.5) was purchased from Gold Biotechnology (St. Louis, MO).

TA2-Gluc was expressed and purified using these reagents: Difco LB Broth Miller (Luria Bertani) (Cat. No. 244620) was purchased from VWR International, LLC (Radnor, PA). Ampicillin sodium (Cat. No. MBPC-1901) purchased from Molecular Biologicals International, Inc., (Irvine, CA). 500 mL 1× PBS (Cat. No. 10010049) and Ni-NTA resin (Cat. No. 88221) was purchased from ThermoFisher Scientific (Waltham, MA). Protein was visualized using mini-PROTEAN TGX Gels (Cat. No. 4561096) (BIORAD Life Sciences, Hercules, CA).

The COVID-19 Incubation buffer (CIB) was composed of 10 mM sodium phosphate dibasic, 2 mM potassium phosphate monobasic, 137 mM sodium chloride, 2.7 mM potassium chloride, 0.05% Tween 20, 1.0% bovine serum albumin, 2% poly (ethylene glycol) 6000 (PEG) at pH 7.4. The coating buffer was composed of 100 mM sodium bicarbonate at pH 9.6. Wash buffer was composed of phosphate buffered saline and Tween 20 (PBST) at pH 7.40. 5  $\mu\text{g mL}^{-1}$  coelenterazine was used as bioluminescent substrate. Blocking buffer PBST (protein-free) (Cat. No. 786-665) was purchased at G-Biosciences (St. Louis, MO). The MOF-ZIF8 solubilizing solution was composed of 200 mM sodium phosphate, and 2 mM EDTA containing 0.01% Tween 20 at pH 5.6.

Cell culture and SARS-CoV-2 pseudovirus propagation was done using MA104 cell line (ATCC CRL-2378.1) purchased from ATCC (Manassas, VA) and medium 199 (1×) (Cat. No. 12340-030) purchased from GIBCO, Thermo Fisher Scientific, (Waltham, MA).

**2.1.2 Apparatus.** For the BIA antibody (Ab) sandwich assay, we used a 96-well, F-bottom (Chimney Well) black, Fluotrac, high-binding, sterile microtiter plate (Cat. No. 82050-046) purchased from Greiner Bio-one (Monroe, NC). BIA assay washing steps were performed using a MultiWash+ plate washer (Molecular Devices LLC., San Jose, CA) using five cycles of 250  $\mu\text{L}$  per well of PBST wash buffer, employing a 10 second shaking step in between each cycle. Light intensity measurements of the bioluminescent reactions were recorded using a CLARIOstar Plus UV/vis spectrometer and luminometer using a fixed gain of 1700 (BMB Labtech, Ortenberg, Germany). Protein concentrations were measured using DeNovix DS-11 Series device that was purchased from DeNovix (Wilmington, DE). The incubation steps were

performed at room temperature using IKA® MS 3 digital shaker at 500 rpm that was purchased from IKA Works, Inc., (Wilmington, NC). Dialysis was performed using 10 000 MWCO Slide-A-lyzer dialysis cassettes G2 (Cat. No. 87730) purchased from ThermoFisher Scientific (Waltham, MA).

Protein expression and purification was done using QSonica sonicator (Qsonica LLC, Newtown, CT), rotary mixer (IKA Trayster Digital) purchased from IKA Works, Inc., (Wilmington, NC) and visualized using SDS page electrophoresis machine purchased from BIORAD Life Sciences, (Hercules, CA).

**2.1.3 Expression and purification of tamavidin2-Gaussia luciferase (TA2-Gluc).** Stock cultures of *Escherichia coli* NEB5-alpha competent cells (New England Biolabs; Ipswich, MA, USA) containing the plasmid TA2-Gluc/pColdI<sup>9</sup> was grown using a sterile Luria Bertani (LB) broth containing 100 mg  $\text{mL}^{-1}$  ampicillin. A Lysis buffer containing 81 mL of 1 M sodium phosphate dibasic and 19 mL of 1 M sodium phosphate monobasic in 900 mL deionized water at pH 7.40 was used for sonication. The cells were sonicated using a micro tip for 20 min on-time; 1 s on-off cycle and purified using immobilized metal affinity chromatography using Ni-NTA resin slurry. The crude mixture was incubated with the resin placed on a rotary mixer for 30 minutes at room temperature. The protein TA2-Gluc was bounded to the Ni-NTA resin and was washed using 10 mL wash buffer containing 50 mM Imidazole twice and passed on a column and the flow-through was collected. The purified protein was eluted with ten (10) aliquots of 1 mL 100 mM Imidazole times and visualized using mini-PROTEAN TGX Gels for SDS-PAGE electrophoresis. After, electrophoresis, pure elution fractions were pooled to give 5–10 mL TA2-Gluc, and excess imidazole was removed by dialysis using a 10 kDa cut-off dialysis cassette. The expressed protein concentration was measured using Pierce 660 protein assay kit according to manufacturer's instructions.

**2.1.4 Encapsulation of TA2-Gluc using the zeolitic imidazolate framework 8 – metal organic framework (ZIF-8-MOF).** In order the encapsulate TA2-Gluc protein with zeolitic imidazolate framework 8, an aliquot of 100  $\mu\text{L}$  of 1  $\mu\text{M}$  TA2-Gluc was mixed with 50  $\mu\text{L}$  of 160 mM zinc acetate and 50  $\mu\text{L}$  of 640 mM 2-methylimidazole solutions. The mixture was then incubated at room temperature. In order to optimize the incubation time for the most efficient incubation, different aliquots of the same solution were incubated at varied time intervals ranging from 10 to 60 minutes. Another tube with only 100  $\mu\text{L}$  of 1  $\mu\text{M}$  TA2-Gluc was prepared to serve as our control. After incubation, the tubes were centrifuged for 10 minutes at 13 000  $\times g$  to collect the ZIF-8 encapsulated TA2-Gluc. The supernatant was removed, and the pellet was dried overnight. Representative samples were stored at various temperatures (25 °C, 4 °C and –20 °C) for future testing.

**2.1.5 Release of the encapsulated TA2-Gluc and bioluminescence activity measurements.** The ZIF-8 crystals were washed 3 times using 1× PBS pH 7.40, vortexed and



centrifuged for 1 minute at  $17000 \times g$ .<sup>22</sup> To release the encapsulated TA2-Gluc, 1 mL of solubilizing solution was added, vortexed thoroughly and incubated at room temperature for 45 minutes. After incubation, the tube was vortexed again and the luminescence signal of the released TA2-Gluc was determined by injecting 100  $\mu\text{L}$  of 5  $\mu\text{g mL}^{-1}$  coelenterazine and measured using a luminometer at 7.40 seconds interval.

#### 2.1.6 Stability assay of TA2-Gluc and MOF-ZIF8 TA2-Gluc.

In order to determine the stability of our reporter fusion protein at ambient temperatures with and without MOF-ZIF8 encapsulation, aliquots of 1000  $\mu\text{L}$  of 1  $\mu\text{M}$  TA2-Gluc solutions were encapsulated as described above. Unencapsulated 1  $\mu\text{M}$  TA2-Gluc was used as controls. These aliquots of the encapsulated fusion proteins were stored at room temperature for up to 6 months, and at predetermined intervals, luminescence emission intensities were measured using a luminometer.

**2.1.7 Incubation time, concentration, binding steps optimization study.** Please see the ESI† section for the assay optimization studies.

**2.1.8 Acquisition, propagation and cultivation of the rVSV-eGFP-SARS-CoV-2 (Pseudovirus).** The 2019 pandemic caused by the severe acute respiratory syndrome coronavirus 2 (SARS-CoV-2) pose threat to the world and still making its way in infecting human causing disease and mortality.<sup>48,49</sup> Due to the virulence and infection caused by this virus, there is a need for a biosafety level 3 confinement.<sup>50,51</sup> To address this problem a pseudo typed virus (Pseudovirus) play an important role in the study and handling of this virus.<sup>49,51</sup> Pseudoviruses are made to provide safer alternative and they are a non-virulent kind of virus that contains the spike protein of SARS-CoV-2 virus.<sup>51</sup> In this study a vesicular stomatitis virus encoding the SARS-CoV-2 spike protein was engineered and kindly donated to our laboratory by Dr. Sean P. J. Whelan of the Department of Molecular Microbiology, Washington University School of Medicine, St Louis, MO, USA. In order to safely perform assay containing the virus, a neutralized high-titer infections molecular clone of SARS-CoV-2 virus (rVSV-eGFP-SARS-CoV-2 (pseudovirus)) was engineered and kindly provided to us by Whelan *et al.*<sup>52</sup> This pseudovirus was propagated and cultivated using MA104 cell line. These cells were grown in a 199 medium until confluent. The T75 flask containing the grown cell line was aspirated and washed using 10 mL  $1 \times$  PBS. A clean 50 mL Falcon tube was prepared and 15  $\mu\text{L}$  of (rVSV-eGFP-SARS-CoV-2) pseudovirus was diluted in 15 mL 199 medium. This was subsequently added to the grown MA104 cell line and incubated at 37 °C (ambient air) and observed for possible cell death due to transfection. After majority of the cells were lysed, the supernatant containing rVSV-eGFP-SARS-CoV-2 were transferred to a clean falcon tube and aliquoted into fractions using a clean cryogenic vial and stored at  $-80^\circ\text{C}$  until needed.<sup>52</sup>

**2.1.9 BIA assay to detect COVID-19 S1 spike antigen and SARS-CoV-2 pseudovirus using the MOFs-TA2Gluc fusion protein.** The wells of a black 96-well F-bottom high binding microtiter plate was coated with 100  $\mu\text{L}$  of 3  $\mu\text{g mL}^{-1}$  capture

antibody in coating buffer and sealed using a transparent ELISA sealing film (BrandTech-Thomas Scientific, Swedesboro, NJ) and incubated overnight at 2–8 °C. The next morning, the coated plate was washed to remove excess coating antibodies and subsequently the wells were incubated with 100  $\mu\text{L}$  COVID-19 S1 spike antigen at varying concentrations ranging from 0.1  $\mu\text{g mL}^{-1}$  to 5  $\mu\text{g mL}^{-1}$  in COVID-19 Incubation Buffer at room temperature using a plate shaker at 500 rpm for 120 minutes. After incubation, the plate was washed and aliquots of 100  $\mu\text{L}$  of 2  $\mu\text{g mL}^{-1}$  Primary antibody in COVID-19 Incubation Buffer was added and incubated at room temperature using a plate shaker at 500 rpm for 120 minutes. After 120 minutes of incubation, the plate was washed and 100  $\mu\text{L}$  of 0.032  $\mu\text{g mL}^{-1}$  biotinylated secondary antibody in COVID-19 Incubation Buffer was added and incubated at room temperature using a plate shaker at 500 rpm for 60 minutes. After another washing step, an aliquot of 100  $\mu\text{L}$  of 1  $\mu\text{M}$  TA2-Gluc in COVID-19 Incubation Buffer was added to the top 4 rows and an aliquot of 100  $\mu\text{L}$  of 1  $\mu\text{M}$  released TA2-Gluc from MOFs-ZIF8 in COVID-19 Incubation Buffer was added to the bottom 4 rows. The plate was incubated at room temperature using a plate shaker at 500 rpm for 10 minutes and washed thereafter. After washing, 100  $\mu\text{L}$  of 5  $\mu\text{g mL}^{-1}$  coelenterazine was added to produce a bioluminescent signal. Our assay was then transitioned from using COVID-19 S1 spike antigen to COVID-19 pseudovirus (rVSV-eGFP-SARS-CoV-2). The BIA was performed following the steps outlined earlier using covid incubation buffer (CIB) and 1:10 dilution of pooled human saliva (PHS) sample containing live SARS-CoV-2 pseudovirus to simulate infection.

**2.1.10 Assay validation study.** The limit of detection and reproducibility of inter and intra assays were performed by repeating the assay steps as described in the section 2.9 for 3 consecutive days in triplicates. The data from these experiments collected and analyzed using GraphPad Prism version 9.2.0 for Mac OS, GraphPad Software, San Diego, CA.

**2.1.11 COVID-19 infected patient sample collection and preparation.** A 500  $\mu\text{L}$  of CIB was placed in a clean extraction buffer tube to serve as sample buffer. A discarded positive nasal swab sample was mixed and dislodged to make a sample slurry. A filtered cap was placed at top of the tube and the sample was squeezed out the tube prior to testing. IRB approval was not sought since the samples were donated and came from a discarded nasal swab, individuals' information was not known.

## 3. Results and discussion

### 3.1 Tamavidin 2 – Gaussia luciferase

A novel genetic fusion protein was created in our laboratory combining a bioluminescent reporter (Gluc) and avidin-like protein, tamavidin, TA2 (TA2-Gluc). This novel genetic fusion protein promises a cost-effective universal reporter based on binding of TA2 to biotin and high luminescent output upon adding the substrate, coelenterazine for Gluc. This fusion can be readily produced using the bacterial expression system in a





reproducible manner. This genetic fusion has 1:1 conjugation ratio and anything biotinylated can be detected using this system as compared to performing chemical conjugation between streptavidin/avidin and a reporter moiety where heterogeneous conjugate mixture is a pitfall.<sup>9</sup>

### 3.2 Room temperature stability of MOF-ZIF 8 encapsulated tamavidin 2 – Gaussia luciferase

We have previously demonstrated that TA2-Gluc, was found to be stable for >6 months at 4 °C.<sup>9</sup> Although this stability is desired, this requires cold chain infrastructure in order to use this fusion protein in assays at point of care or resource limited settings. To be able to store a protein-based reagent at room temperature is very desirable, however, our fusion protein loses its activity in 6 to 8 hours at room temperature. In order to address this problem, we decided to use metal organic framework encapsulation to stabilize TA2-Gluc. It has been shown in the literature that metal organic framework can be used to stabilize biological molecules very efficiently.<sup>14,20,23</sup> For example, zinc ions coupled with methyl-imidazole molecules forms a cage-like encapsulation that traps the fusion protein (Fig. 1A), stabilizing the protein in the process. When needed, the encapsulated protein can be released from this cage like structure by solubilizing the MOFs-ZIF 8 using a slightly acidic

buffer (pH ~6) to shift the ionization of the imidazole moiety and thereby disrupting the Zn–imidazole interactions, and EDTA to chelate the released zinc ions (Fig. 1B). TA2-Gluc fusion protein, once released, can then react with its substrate, coelenterazine, to produce a bright luminescence (Fig. 1C). To demonstrate that this particular MOF encapsulated TA2-Gluc protein is more stable than the unencapsulated fusion protein, an equimolar solution of TA2-Gluc encapsulated with MOF-ZIF 8 was tested for stability and compared to native TA2-Gluc. The bioluminescence activity was used as the benchmark for stability, and we demonstrated that TA2-Gluc preserved by encapsulation exhibited higher luminescence intensity when compared to the native TA2-Gluc (Fig. 2A). Encapsulation or immobilization of various proteins on surfaces have been previously shown to improve protein activity and hence our observation of higher luminescence upon encapsulation is not surprising.<sup>18,53</sup> The stability of the encapsulated fusion protein at various temperatures (room temperature (RT), 4 °C and –20 °C) was monitored and indicated that we can preserve this fusion protein with MOF-ZIF 8 (Fig. 2B) in any of the tested temperatures. We monitored the stability of this MOF-ZIF 8 fusion protein and demonstrated its stability for up to 6 months at ambient storage conditions that can be potentially utilized as part of an assay in a point-of-care setting (Fig. 1C).

### 3.3 Optimization and evaluation of MOFs-ZIF 8 encapsulated TA2-Gluc in a bioluminescent immuno-assay (BIA)

BIA are an excellent assay system for the detection of biomolecules<sup>54</sup> as they afford high sensitivity and specificity. To further expand on their potential applications, we prepared

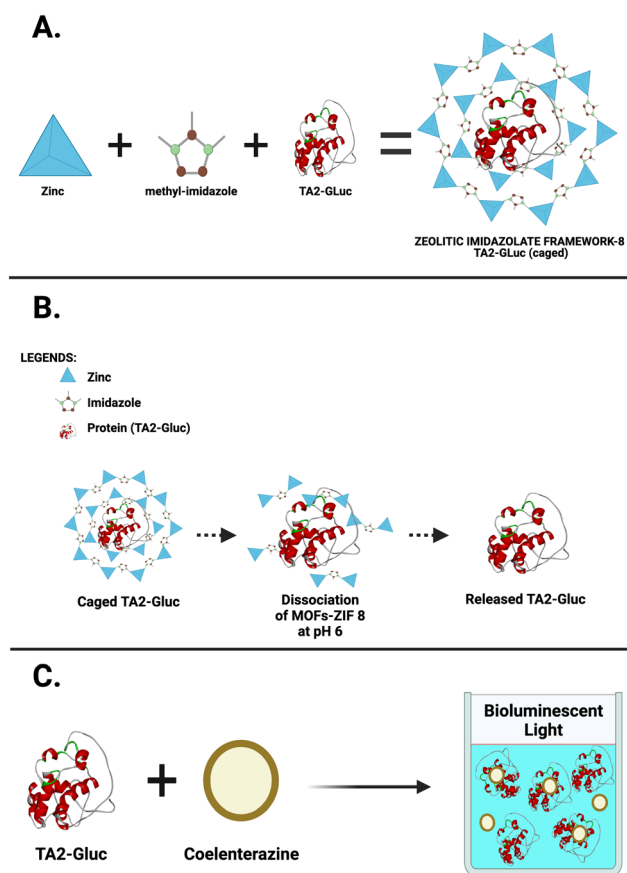


**Fig. 1** Metal organic frameworks (ZIF-8) A. Encapsulation of TA2-Gluc. B. TA2-Gluc release at pH 6. C. TA2-Gluc with its substrate coelenterazine producing bioluminescent signal.

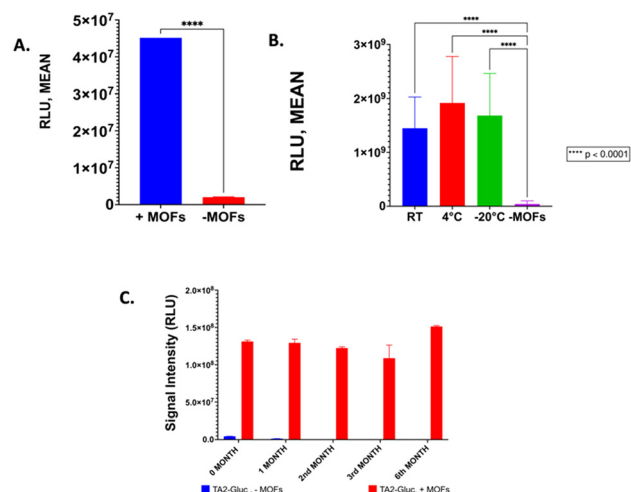


**Fig. 2** Bioluminescent activity plots for encapsulated and unencapsulated fusion protein. A. Bioluminescent light intensity of the fusion protein TA2-Gluc (–MOFs) compared to TA2-Gluc encapsulated using MOFs-ZIF 8 (+MOFs) day after the encapsulation. B. TA2-Gluc with MOF-ZIF 8 at various temperatures (RT, 4 °C, and –20 °C) as compared to no encapsulation (–MOFs) kept at 4 °C, day after the preparation. C. Encapsulation stability testing of the fusion protein TA2-Gluc compared to native TA2-Gluc over time stored at room temperature. Data are the mean of four replicates. Error bars represents standard error of the mean, and some are obstructed by the data points.



room temperature stable universal bioluminescent reporter, MOF-ZIF 8 TA2-Gluc and showed its application in a BIA system. In this study, we used SARS-CoV-2 spike antigen as the model analyte for the design of BIA since this antigen is of importance in the detection of virus causing COVID-19 pandemic. The schematic for the BIA assay is depicted in Fig. 3A.

For this assay, COVID-19 S1 spike antigen is first captured by SARS-CoV-2 spike antibody that is coated into the wells of the microtiter plate. When the antigen is captured, the primary antibody against the COVID-19 S1 spike antigen will bind to spike antigen forming an antibody sandwich. Once this antibody sandwich is formed, a biotinylated secondary antibody is added, which binds to the Fc receptor of the primary

antibody. The reporter, MOF encapsulated TA2-Gluc binds to the biotin and a measurable signal is produced upon adding the substrate for the Gluc, coelenterazine. The signal produced is correlated to the amount of spike antigen and in turn the presence of SARS-CoV-2 viral copies present in the sample. The availability of this MOF-ZIF8 encapsulated fusion protein could be an avenue for a new and more stable reporters that can be used to detect target analytes of interest potentially in immunoassays applicable to a point-of-care setting. Moreover, since we have demonstrated its stability at room temperature for over six months, this MOF ZIF8 encapsulated protein can be shipped across the world without the need for a cold chain infrastructure. We believe this is a tremendous advantage for

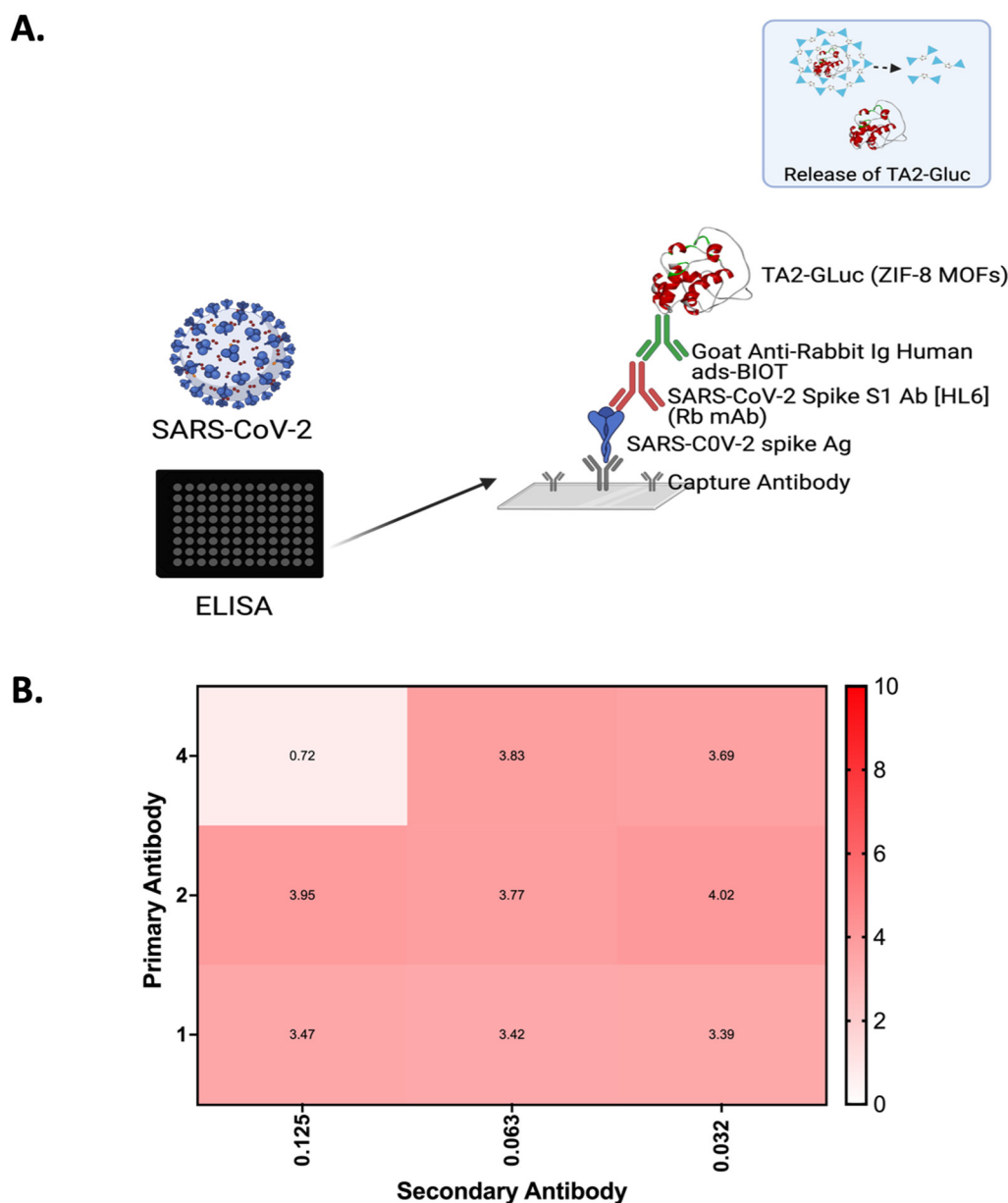


**Fig. 3** Schematic showing bioluminescent immunoassay steps. A. BIA using the MOF-ZIF 8 TA2-Gluc as reporter for COVID 19 S1 spike antigen detection. B. Checkerboard optimization assay for the primary (SARS-CoV-2 spike S1 antibody [HL6] Rb mAb,  $\mu\text{g mL}^{-1}$ ) and secondary (goat anti-rabbit Ig human ads-BIOT,  $\mu\text{g mL}^{-1}$ ) antibody pairs. The results were presented as a heat map plot with reported signal to noise (S/N) ratio.



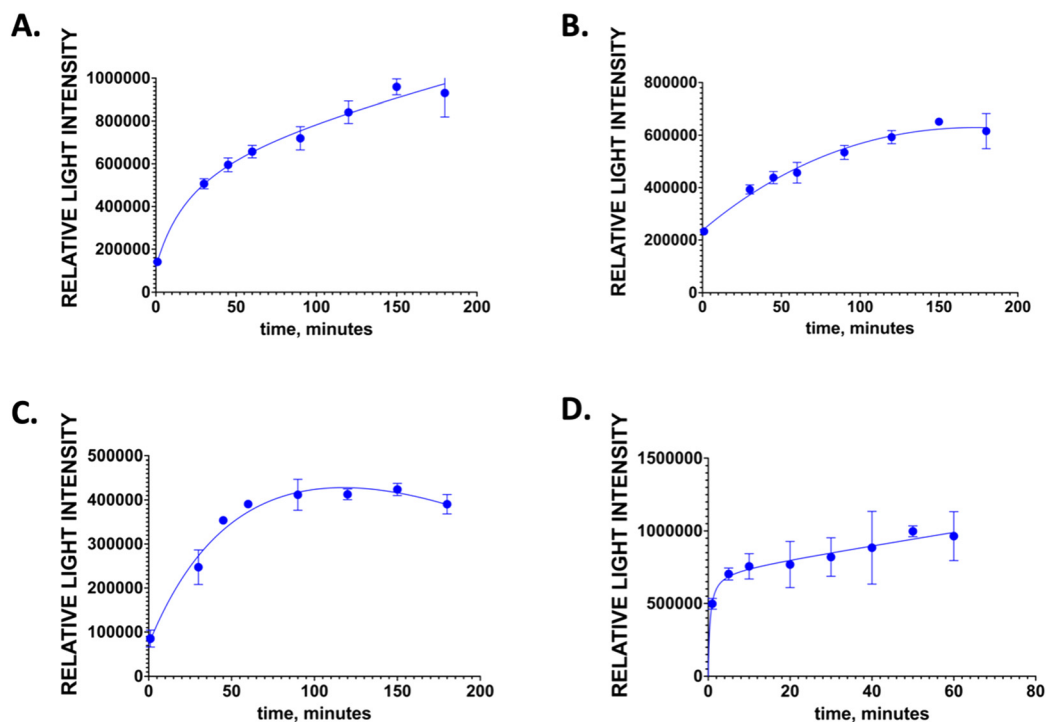


**Fig. 4** Time optimization for each step of the BIA. A. COVID-19 S1 spike antigen incubation time. B. Primary antibody incubation time. C. Biotinylated secondary antibody incubation time and D. MOF-ZIF 8 TA2-Gluc incubation time. Data are the mean of four replicates. Error bars represents standard error of the mean, and some are obstructed by the data points.

low resource countries. A checkerboard assay was done to optimize the concentration of the antibody pair ( $2 \mu\text{g mL}^{-1}$ , primary antibody, and  $0.32 \mu\text{g mL}^{-1}$  biotinylated secondary antibody) to improve the sensitivity of the assay. Signal to noise ratio was calculated by dividing the light intensity of those that have the COVID-19 S1 spike antigen (positive control) to the light intensity by those that do not have the COVID-19 s1 spike antigen (negative control) (Fig. 3B). The blocking conditions for this assay was optimized to reduce the non-specific binding. Several different blocking buffers and buffering conditions were tested, and we found that the blocking step is not necessary for this assay. The optimized incubation time for the antigen, primary antibody, biotinylated secondary antibody, and the reporter MOF-ZIF8 TA2-Gluc time are summarized in Fig. 4 and Table 1. We optimized the time of incubation to minimize overall assay time without compromising the sensitivity of the assay. The optimized incubation times and concentrations are listed in Table 1. Overall, the total assay time for the laboratory-based BIA was less than 6 hours. This is comparable to other laboratory-based immunoassays reported in the literature. The

signal generation using MOF-ZIF 8 TA2-Gluc as a reporter is rapid within 3 s and provide a great addition to the existing reporters that are currently available on the market as a room temperature stable reporter.

### 3.4 Dose-response curve for SARS-CoV-2 S1 spike antigen and assay reproducibility

Using the optimized BIA conditions we generated a dose-response curve by varying SARS-CoV-2 spike antigen to obtain a detection limit. First, we compared the performance of the assay using TA2-Gluc without any MOFs encapsulation and compared the dose-response curve with the MOF encapsulated TA2-Gluc. We observed that the MOF encapsulated fusion protein gave similar results as compared to using the fusion protein alone (Fig. 5A). Similar dose-response curve was obtained while using MOFs encapsulated TA2-Gluc stored at room temperature over a longer period (Fig. 5A). This indicates that encapsulation of the fusion protein does not affect the assay performance while affording better stability to the reporter protein. Moreover, the room-temperature stored protein can be used as a reporter without affecting the performance of the assay. We also performed a reproducibility assay using the optimal conditions. For this purpose, three separate assays were performed on three separate days and the results were compared. Fig. 5B shows day to day reproducibility. There was no significant difference in the curves obtained over three days and the limit of detection of  $0.26 \mu\text{g mL}^{-1}$  was obtained on all three days. The

**Table 1** Optimization of the components concentration and incubation time

Components	Concentrations	Incubation time
Capture antibody	$3 \mu\text{g mL}^{-1}$	Overnight
COVID-19 spike Ag	$2 \mu\text{g mL}^{-1}$	120 minutes
Primary antibody	$2 \mu\text{g mL}^{-1}$	120 minutes
Biotinylated secondary antibody	$0.032 \mu\text{g mL}^{-1}$	60 minutes
ZIF-8 encapsulated TA2-Gluc	$1 \mu\text{M}$	10 minutes



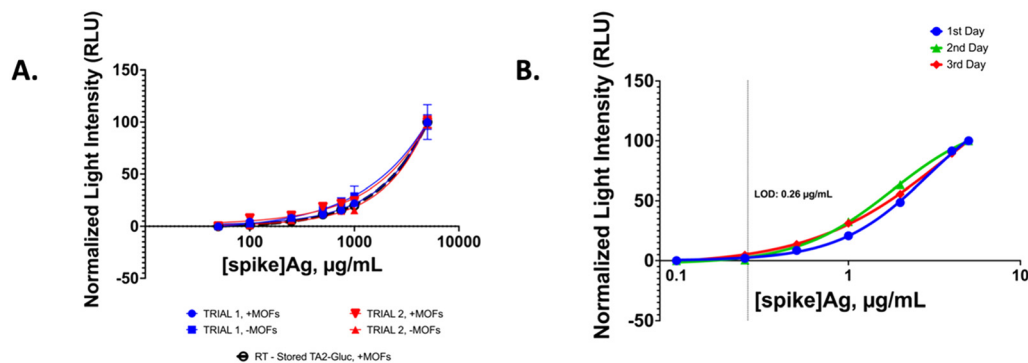


Fig. 5 A. Dose-response curve obtained for the SARS-CoV-2 spike antigen using TA2-Gluc fusion reporter with and without encapsulation using MOFs and using long-term stored MOFs encapsulate TA2-Gluc. B. Inter-intra assay study to determine reproducibility and limit of detection (LOD) of BIA assay in detecting COVID-19 S1 spike antigen using our laboratory created fusion-protein TA2-Gluc preserved using MOFs-ZIF 8.

detection limit was obtained by interpolation from the GraphPad Prism software using the following formula  $\text{LOD} = S_B + 3 \times \text{SD}_B$  where  $S_B$  and  $\text{SD}_B$  are the mean and the standard deviation of the blank signals, respectively.<sup>55</sup>

### 3.5 Detection of SARS-COV-2 pseudo virus in a physiological fluid and SARS-CoV-2 Ag in nasal swab samples of infected individuals

To demonstrate that we can use the BIA developed for the detection of virus if present in the physiological fluid we performed analysis using spiked pooled human saliva (PHS) and nasopharyngeal swab samples. We compared the

performance in these samples with SARS-CoV-2 pseudovirus spiked into the COVID incubation buffer (CIB). Pseudovirus was used since it contains the spike protein of the virus but does not have the virulence and hence it can be safely handled. Different known copies per mL of pseudovirus were spiked into the CIB and PHS samples. BIA was performed following the optimized conditions and using these spiked samples (Fig. 6). A limit of detection of  $2.94 \times 10^4$  copies per mL in CIB samples,  $7.33 \times 10^4$  copies per mL in PHS samples and  $4.24 \times 10^5$  for nasopharyngeal swab medium was obtained. For both physiological fluids 1:10 dilution showed similar detection limit as the buffer. The levels of viral copies reported in saliva and nasopharyngeal swabs range from  $10^4$

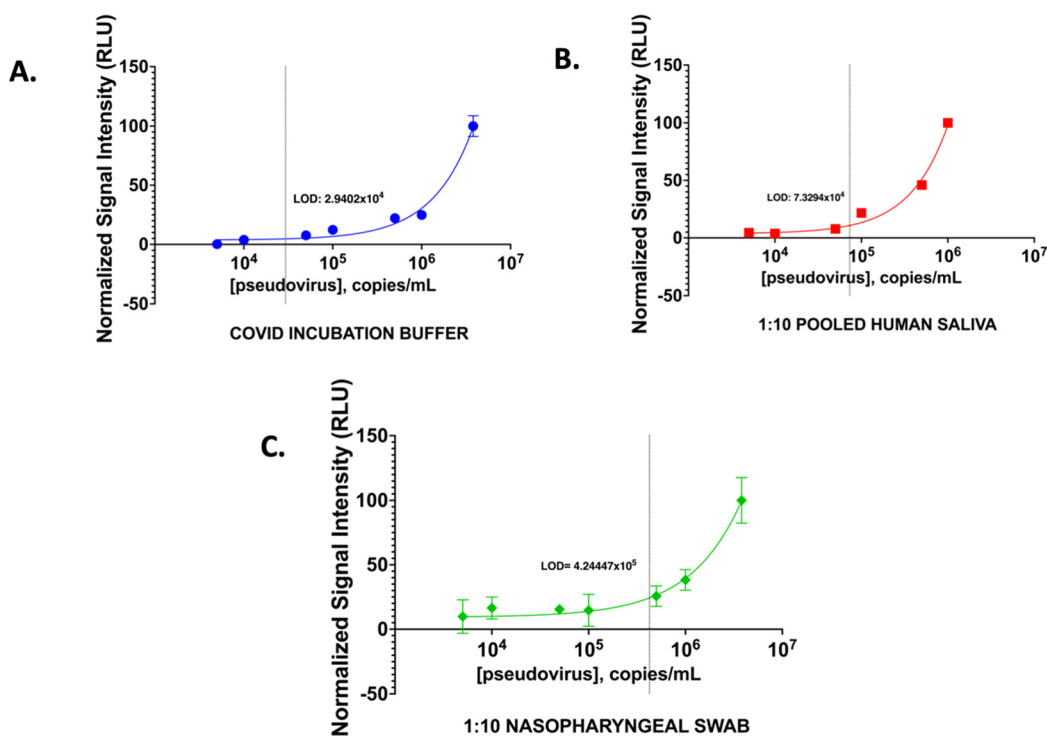


Fig. 6 A. Dose-response curve obtained for rVSV-SARS-CoV-2 virus spiked into CIB. B. Dose-response curve obtained for rVSV-SARS-CoV-2 virus spiked into 1:10 pooled human saliva (PHS). C. Dose-response curve obtained for rVSV-SARS-CoV-2 virus spiked into 1:10 nasopharyngeal swab medium. Data are the mean of four replicates. Error bars represents standard error of the mean, and some are obstructed by the data points.





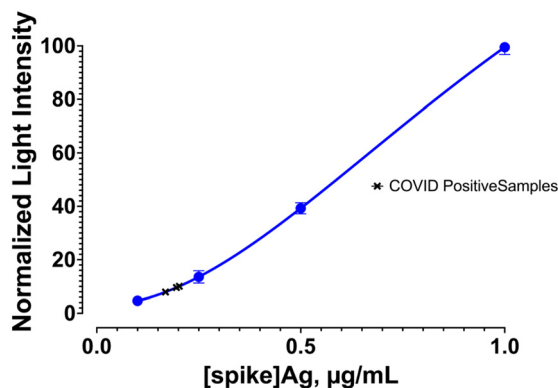


Fig. 7 SARS-CoV-2 spike Ag detected in nasal swab samples.

to  $10^7$  copies per mL in infected individuals<sup>56,57</sup> with symptoms. Although, RT-PCR-based analysis can yield much lower limit of detection due to the amplification process and allow early identification of COVID-19 infection, currently available immunoassay-based methods are able to diagnose symptomatic patients with similar detection limits as demonstrated in our assay since the sensitivity of the assays are dependent on binding constants of the antibodies employed and there is no amplification like in a molecular test. To show that our assay can detect COVID-19 positive patients similar to the currently available immunoassay tests, we evaluated nasal swab samples of individuals who were diagnosed with COVID-19 using the rapid antigen test. The bioluminescent assay using the fusion protein TA2-Gluc can detect viral spike antigen at concentration above the detection limit and correctly identified all (3) tested positive samples as positive in the assay (Fig. 7). This performance is similar to the currently available antigen tests.

## 4. Conclusions

Encapsulation of biological materials such as DNA, RNA, and proteins within metal organic frameworks improve their stability significantly. MOF encapsulated biologics are stable at room temperature therefore they do not require any refrigeration or cold-chain infrastructure. Since refrigeration is not required to store and ship these materials, these assays can be useful in low resource settings where access to power is very limited. In this study, we have encapsulated a fusion protein between tamavidin2 and Gaussia luciferase, which can be used as a universal reporter based on biotin-tamavidin-binding and was demonstrated that it can be stored at room temperature up to 6 months. Using MOF to enclose and encapsulate the bioluminescent protein allows us to store it for a longer period of time which provides a comparable or better preservation efficacy than freezing liquid samples at  $-20$  °C. This is an energy-efficient and environmentally friendly approach that works to reduce the need for cold chain and temperature-controlled handling and testing of biospecimens.<sup>24</sup> This encapsulated fusion protein then can be released, on demand, from its metal organic

framework, and used as a reporter in bioluminescent assays. We also showed that this reporter can be used in the design of bioluminescent immunoassay by using SARS-CoV-2 spike antigen as a model target and showed its usefulness in detecting virus in real samples from the physiological fluids similar to the currently available antigen tests.

## Conflicts of interest

There are no conflicts to declare.

## Acknowledgements

The authors would like to thank NIGMS (R01GM114321 and R01GM127706), the National Science Foundation (CBET-1841419/EAGER-2041413), Dr. John T. McDonald Foundation, and University of Miami CTSI for funding support. S. D. thanks the Miller School of Medicine of the University of Miami for the Lucille P. Markey Chair in Biochemistry and Molecular Biology. The authors would like to thank Dr. Sean P. J. Whelan of Washington University School of Medicine for providing us the rVSV-SARS-CoV-2 viral clone.

## References

- O. Villard, *et al.*, Evaluation of the usefulness of six commercial agglutination assays for serologic diagnosis of toxoplasmosis, *Diagn. Microbiol. Infect. Dis.*, 2012, **73**(3), 231–235.
- S. Edouard, *et al.*, Evaluating the serological status of COVID-19 patients using an indirect immunofluorescent assay, France, *Eur. J. Clin. Microbiol. Infect. Dis.*, 2021, **40**(2), 361–371.
- A. K. Malan, *et al.*, Detection of IgG and IgM to West Nile virus: development of an immunofluorescence assay, *Am. J. Clin. Pathol.*, 2003, **119**(4), 508–515.
- H. R. Hill and J. M. Matsen, Enzyme-linked immunosorbent assay and radioimmunoassay in the serologic diagnosis of infectious diseases, *J. Infect. Dis.*, 1983, **147**(2), 258–263.
- D. N. Sharmila, Serological Investigation in Viral Infection. A Review, *Ann. Romanian Soc. Cell Biol.*, 2021, 826–840.
- S. Aydin, A short history, principles, and types of ELISA, and our laboratory experience with peptide/protein analyses using ELISA, *Peptides*, 2015, **72**, 4–15.
- M. E. Goldberg and L. Djavadi-Ohanian, Methods for measurement of antibody/antigen affinity based on ELISA and RIA, *Curr. Opin. Immunol.*, 1993, **5**(2), 278–281.
- J. M. Faupel-Badger, *et al.*, Comparison of liquid chromatography-tandem mass spectrometry, RIA, and ELISA methods for measurement of urinary estrogens, *Cancer Epidemiol. Biomark. Prev.*, 2010, **19**(1), 292–300.
- D. B. Broyles, *et al.*, Facile Synthesis and Characterization of a Novel Tamavidin-Luciferase Reporter Fusion Protein for Universal Signaling Applications, *Adv. Biosyst.*, 2020, **4**(4), 1900166.
- R. Ladj, *et al.*, Polymer encapsulation of inorganic nanoparticles for biomedical applications, *Int. J. Pharm.*, 2013, **458**(1), 230–241.



- 11 E. Villemin, *et al.*, Polymer encapsulation of ruthenium complexes for biological and medicinal applications, *Nat. Rev. Chem.*, 2019, **3**(4), 261–282.
- 12 R. J. Kuppler, *et al.*, Potential applications of metal-organic frameworks, *Coord. Chem. Rev.*, 2009, **253**(23–24), 3042–3066.
- 13 G. Lu, *et al.*, Imparting functionality to a metal-organic framework material by controlled nanoparticle encapsulation, *Nat. Chem.*, 2012, **4**(4), 310–316.
- 14 C. Wang, *et al.*, Metal-Organic Framework Encapsulation Preserves the Bioactivity of Protein Therapeutics, *Adv. Healthcare Mater.*, 2018, **7**(22), 1800950.
- 15 S. Kitagawa, Metal-organic frameworks (MOFs), *Chem. Soc. Rev.*, 2014, **43**(16), 5415–5418.
- 16 J. Zhuang, A. P. Young and C. K. Tsung, Integration of biomolecules with metal-organic frameworks, *Small*, 2017, **13**(32), 1700880.
- 17 L. E. Kreno, *et al.*, Metal-organic framework materials as chemical sensors, *Chem. Rev.*, 2012, **112**(2), 1105–1125.
- 18 Q.-L. Zhu and Q. Xu, Metal-organic framework composites, *Chem. Soc. Rev.*, 2014, **43**(16), 5468–5512.
- 19 W. Liang, *et al.*, Metal-organic framework-based enzyme biocomposites, *Chem. Rev.*, 2021, **121**(3), 1077–1129.
- 20 Y. Feng, *et al.*, Antibodies@ MOFs: an in vitro protective coating for preparation and storage of biopharmaceuticals, *Adv. Mater.*, 2019, **31**(2), 1805148.
- 21 Y. Sun, *et al.*, Metal-organic framework nanocarriers for drug delivery in biomedical applications, *Nano-Micro Lett.*, 2020, **12**(1), 1–29.
- 22 K. Liang, *et al.*, Biomimetic mineralization of metal-organic frameworks as protective coatings for biomacromolecules, *Nat. Commun.*, 2015, **6**(1), 1–8.
- 23 C. Wang, *et al.*, Metal-organic framework encapsulation for biospecimen preservation, *Chem. Mater.*, 2018, **30**(4), 1291–1300.
- 24 X. Lin, *et al.*, Encapsulation of strongly fluorescent carbon quantum dots in metal-organic frameworks for enhancing chemical sensing, *Anal. Chem.*, 2014, **86**(2), 1223–1228.
- 25 D. Zou, D. Liu and J. Zhang, From Zeolitic Imidazolate Framework-8 to Metal-Organic Frameworks (MOF s): Representative Substance for the General Study of Pioneering MOF Applications, *Energy Environ. Mater.*, 2018, **1**(4), 209–220.
- 26 M. G. Campbell, *et al.*, Chemiresistive sensor arrays from conductive 2D metal-organic frameworks, *J. Am. Chem. Soc.*, 2015, **137**(43), 13780–13783.
- 27 D. Wang, D. Jana and Y. Zhao, Metal-organic framework derived nanozymes in biomedicine, *Acc. Chem. Res.*, 2020, **53**(7), 1389–1400.
- 28 H. Li, *et al.*, Design and synthesis of an exceptionally stable and highly porous metal-organic framework, *Nature*, 1999, **402**(6759), 276–279.
- 29 M. Ataei-Kachouei, S. Shahrokhian and M. Ezzati, Bimetallic CoZn-MOFs easily derived from CoZn-LDHs, as a suitable platform in fabrication of a non-enzymatic electrochemical sensor for detecting glucose in human fluids, *Sens. Actuators, B*, 2021, 130254.
- 30 Z. Sun, *et al.*, Sensor array for rapid pathogens identification fabricated with peptide-conjugated 2D metal-organic framework nanosheets, *Chem. Eng. J.*, 2021, **405**, 126707.
- 31 P. Sharanyakanth and M. Radhakrishnan, Synthesis of metal-organic frameworks (MOFs) and its application in food packaging: A critical review, *Trends Food Sci. Technol.*, 2020, **104**, 102–116.
- 32 Y.-R. Lee, *et al.*, ZIF-8: A comparison of synthesis methods, *Chem. Eng. J.*, 2015, **271**, 276–280.
- 33 H. K. Jeong, Metal-organic framework membranes: Unprecedented opportunities for gas separations, *AIChE J.*, 2021, **67**(6), e17258.
- 34 Z. Lai, Development of ZIF-8 membranes: opportunities and challenges for commercial applications, *Curr. Opin. Chem. Eng.*, 2018, **20**, 78–85.
- 35 Y.-R. Lee, J. Kim and W.-S. Ahn, Synthesis of metal-organic frameworks: A mini review, *Korean J. Chem. Eng.*, 2013, **30**(9), 1667–1680.
- 36 C. Wang, *et al.*, Metal-Organic Framework as a Protective Coating for Biodiagnostic Chips, *Adv. Mater.*, 2017, **29**(7), 1604433.
- 37 C. Doonan, *et al.*, Metal-organic frameworks at the biointerface: synthetic strategies and applications, *Acc. Chem. Res.*, 2017, **50**(6), 1423–1432.
- 38 Q. Jiang, *et al.*, Rapid, point-of-care, paper-based plasmonic biosensor for Zika virus diagnosis, *Adv. Biosyst.*, 2017, **1**(9), 1700096.
- 39 Y. Takakura, *et al.*, Tamavidin, a versatile affinity tag for protein purification and immobilization, *J. Biotechnol.*, 2010, **145**(4), 317–322.
- 40 Y. Takakura, *et al.*, Lentiavidins: Novel avidin-like proteins with low isoelectric points from shiitake mushroom (*Lentinula edodes*), *J. Biosci. Bioeng.*, 2016, **121**(4), 420–423.
- 41 R. F. Delgadillo, *et al.*, Detailed characterization of the solution kinetics and thermodynamics of biotin, biocytin and HABA binding to avidin and streptavidin, *PLoS One*, 2019, **14**(2), e0204194.
- 42 Z. M. Kaskova, A. S. Tsarkova and I. V. Yampolsky, 1001 lights: luciferins, luciferases, their mechanisms of action and applications in chemical analysis, biology and medicine, *Chem. Soc. Rev.*, 2016, **45**(21), 6048–6077.
- 43 B. Hu, *et al.*, Characteristics of SARS-CoV-2 and COVID-19, *Nat. Rev. Microbiol.*, 2021, **19**(3), 141–154.
- 44 M. A. Shereen, *et al.*, COVID-19 infection: Origin, transmission, and characteristics of human coronaviruses, *J. Adv. Res.*, 2020, **24**, 91.
- 45 L. Morawska, *et al.*, How can airborne transmission of COVID-19 indoors be minimised?, *Environ. Int.*, 2020, **142**, 105832.
- 46 Q. Liu, K. Xu, X. Wang and W. Wang, From Sars to Covid-19: What Lessons Have We Learned?, *J. Infect. Public Health*, 2020, **13**(11), 1611–1618.
- 47 T. P. Velavan and C. G. Meyer, The COVID-19 epidemic, *Trop. Med. Int. Health*, 2020, **25**(3), 278.
- 48 M. M. Lamers and B. L. Haagmans, SARS-CoV-2 pathogenesis, *Nat. Rev. Microbiol.*, 2022, **20**(5), 270–284.



- 49 S.-H. Tseng, *et al.*, A novel pseudovirus-based mouse model of SARS-CoV-2 infection to test COVID-19 interventions, *J. Biomed. Sci.*, 2021, **28**(1), 1–8.
- 50 J. Malicoat, S. Manivasagam, S. Zuñiga, I. Sola, D. McCabe, L. Rong, S. Perlman, L. Enjuanes and B. Manicassamy, Development of a Single-Cycle Infectious SARS-CoV-2 Virus Replicon Particle System for Use in Biosafety Level 2 Laboratories, *J. Virol.*, 2022, **96**(3), e01837-21.
- 51 M. Chen and X.-E. Zhang, Construction and applications of SARS-CoV-2 pseudoviruses: a mini review, *Int. J. Biol. Sci.*, 2021, **17**(6), 1574.
- 52 J. B. Case, P. W. Rothlauf, R. E. Chen, Z. Liu, H. Zhao, A. S. Kim, L. M. Bloyet, Q. Zeng, S. Tahan, L. Droit and M. X. G. Ilagan, Neutralizing antibody and soluble ACE2 inhibition of a replication-competent VSV-SARS-CoV-2 and a clinical isolate of SARS-CoV-2, *Cell Host Microbe*, 2020, **28**(3), 475–485.
- 53 H. Xia, *et al.*, Metal-organic frameworks: a potential platform for enzyme immobilization and related applications, *Front. Bioeng. Biotechnol.*, 2020, **8**, 695.
- 54 A. Fleiss and K. S. Sarkisyan, A brief review of bioluminescent systems (2019), *Curr. Genet.*, 2019, **65**(4), 877–882.
- 55 X. Wan, *et al.*, Cascaded amplifying circuits enable ultrasensitive cellular sensors for toxic metals, *Nat. Chem. Biol.*, 2019, **15**(5), 540–548.
- 56 J. Zhu, *et al.*, Viral dynamics of SARS-CoV-2 in saliva from infected patients, *J. Infect.*, 2020, **81**(3), e48–e50.
- 57 Y. Pan, *et al.*, Viral load of SARS-CoV-2 in clinical samples, *Lancet Infect. Dis.*, 2020, **20**(4), 411–412.

